AGU PUBLICATIONS

Geophysical Research Letters

RESEARCH LETTER
10.1002/2017GL073585

Key Points:
- Novel laboratory measurements of ice melt rates reveal a nonlinear dependence on flow speed, associated with detachment of side melt plumes
- In a homogeneous flow, meltwater spreads at the surface for attached melt plumes and mixes as deep as the ice draft for detached plumes
- Including this regime transition in a parameterization of iceberg side melt improves agreement with melt observations in a Greenland fjord

Supporting Information:
- Supporting Information S1

Correspondence to:
A. FitzMaurice,
apf@princeton.edu

Citation:
FitzMaurice, A., C. Cenedese, and F. Straneo (2017), Nonlinear response of iceberg side melting to ocean currents, *Geophys. Res. Lett.*, *44*, 5637–5644, doi:10.1002/2017GL073585.

Received 23 MAR 2017
Accepted 31 MAY 2017
Accepted article online 8 JUN 2017
Published online 12 JUN 2017

Nonlinear response of iceberg side melting to ocean currents

A. FitzMaurice[1], C. Cenedese[2], and F. Straneo[2]

[1]Program in Atmospheric and Oceanic Sciences, Princeton University, Princeton, New Jersey, USA, [2]Woods Hole Oceanographic Institution, Woods Hole, Massachusetts, USA

Abstract Icebergs calving into Greenlandic Fjords frequently experience strongly sheared flows over their draft, but the impact of this flow past the iceberg is not fully captured by existing parameterizations. We present a series of novel laboratory experiments to determine the dependence of submarine melting along iceberg sides on a background flow. We show, for the first time, that two distinct regimes of melting exist depending on the flow magnitude and consequent behavior of melt plumes (side-attached or side-detached), with correspondingly different meltwater spreading characteristics. When this velocity dependence is included in melt parameterizations, melt rates estimated for observed icebergs in the attached regime increase, consistent with observed iceberg submarine melt rates. We show that both attached and detached plume regimes are relevant to icebergs observed in a Greenland fjord. Further, depending on the regime, iceberg meltwater may either be confined to a surface layer or distributed over the iceberg draft.

1. Introduction

With rising global temperatures there has been an observed increase in the discharge of ice from the Antarctic and Greenland ice sheets [*Bamber and Aspinall*, 2013; *Rignot et al.*, 2011]. This trend has motivated a focus on the study of icebergs, which act as conduits for transporting freshwater from the ice sheet margins to the ocean as they are carried away from their sources and melt. Where and how these icebergs melt has the potential to affect both ocean stratification and local productivity (through, for example, the upwelling of nutrient-rich water) [*Smith et al.*, 2007; *Duprat et al.*, 2016]. Despite the regional nature of such effects, they have implications for the large-scale ocean circulation and sequestration of carbon by the ocean [e.g., *Böning et al.*, 2016; *Sgubin et al.*, 2017], which makes understanding iceberg melting a priority in the context of a warming climate.

Analogously to tidewater glaciers, one primary mechanism involved in iceberg melt is meltwater plumes rising along the ice-ocean interface. In a recent study by *Yankovsky and Yashayaev* [2014], detailed surveys of two Greenlandic icebergs revealed that icebergs subject to different oceanic and atmospheric conditions may have melt plumes with very different surface expressions. Yet to date, parameterizations of iceberg melt in climate models have neglected the influence of melt plumes on the Submarine Melt Rate (SMR) and the location where meltwater is discharged in the water column. Recent work indicating that icebergs in Greenlandic fjords are frequently subject to strongly vertically sheared flows [*FitzMaurice et al.*, 2016] further highlights the need for a consistent parameterization of iceberg melt that takes the influence of ocean currents on melt plumes into account. In addition to its effect on SMR, flow past an iceberg is anticipated to alter the melt plume mixing and entrainment, and hence the intrusion depth of the modified meltwater layer.

In what follows we use, for the first time, laboratory experiments to understand the effect of flow past an iceberg on iceberg melt plumes and the distribution of meltwater in the water column. The current state of scientific knowledge about submarine iceberg melt is summarized in section 2, the original experiments carried out to deduce the effect of flow past an iceberg on iceberg side melt plumes are described in section 3, and their results are described in section 4. An updated parameterization of iceberg side melt accounting for side melt plumes is introduced in section 5.1 and is applied to observed icebergs in section 5.2. Discussion and conclusions follow in sections 6 and 7.

2. Background

Our existing understanding of icebergs' submarine melting is derived from a combination of observations, laboratory experiments, and mathematical modeling. Studies of individual icebergs and iceberg distributions have allowed ballpark estimates of their melt rate and deterioration as a function of ocean temperature [*Budd et al.*, 1980; *Hobson et al.*, 2011], and more recently, satellite altimetry has been used to constrain iceberg mass loss over time [*Enderlin and Hamilton*, 2014; *Enderlin et al.*, 2016]. Hydrographic surveys conducted near melting icebergs have shown that icebergs can locally influence ocean properties, with iceberg melt plumes displaying enhanced upwelling and cooled temperatures [*Josberger and Neshyba*, 1980; *Helly et al.*, 2010; *Stephenson et al.*, 2015]. Laboratory experiments have investigated in depth the influence of vertical temperature and salinity gradients on SMR, the shape evolution of melting ice, and the distribution of meltwater assuming no background flow [*Huppert and Turner*, 1980; *Russell-Head*, 1980; *Gade*, 1993; *McConnochie and Kerr*, 2016].

Observational and experimental findings have informed the development of parameterizations of iceberg melt [*Weeks and Campbell*, 1973; *Neshyba and Josberger*, 1980; *El-Tahan et al.*, 1987], used to predict the large-scale distribution of meltwater along modeled iceberg trajectories [*Bigg et al.*, 1997; *Gladstone et al.*, 2001; *Kubat et al.*, 2007]. Current parameterizations of iceberg side melt M_s separate melting into forced convection M_b due to heat exchange driven by flow past the iceberg, and a velocity-independent buoyant convection term M_v that is small in comparison to M_b [*Savage*, 2001]. Some numerical models apply M_v to calculate side melt and thus have an entirely velocity-independent side melt rate [*Martin and Adcroft*, 2010], while others, in units of m d^{-1}, take

$$M_s = M_v + M_b, \tag{1}$$

$$= \left(aT_o + bT_o^2\right) + K\,|\vec{u}_i - \vec{u}_o|^{0.8}\,\frac{T_o - T_i}{L^{0.2}} \tag{2}$$

for water temperature T_o, ice temperature T_i, L being the iceberg length, and $|\vec{u}_i - \vec{u}_o|$ the relative speed between the iceberg and the water. Here $a = 7.62 \times 10^{-3}$, $b = 1.29 \times 10^{-3}$ [*Neshyba and Josberger*, 1980], and K is a function of the water temperature, generally taken as 0.58 for oceanic conditions [*Weeks and Campbell*, 1973] (see Supporting Information for details).

The form of M_v was obtained from an empirical fit to observations of icebergs melting in different temperature water [*Neshyba and Josberger*, 1980], while M_b is derived from the theory of flow past an isothermal plate [*Weeks and Campbell*, 1973], but there has been no formal consideration given to whether M_v and M_b are additive or to the effect of vertical melt plumes parallel to the ice. Work has been done to explicitly account for melt plumes in the case of melt under ice shelves and at the faces of tidewater glaciers, for which the canonical parameterization is the "three-equation model" of *Holland and Jenkins* [1999]. In this parameterization it is found that the velocity along the ice face (corresponding to the melt plume velocity) can act as a strong control on the melt rate, with fast melt plumes inducing much more melting than slow melt plumes [*Sciascia et al.*, 2013]. While incorporating a velocity that is parallel to the ice face (the rising buoyant plume's velocity), this parameterization does not allow for lateral flow around the ice and perpendicular to the melt plume. It consequently does not account for the influence of a background advective velocity on melting, either directly or via the flow's interactions with melt plumes. It is the effect of such a velocity that is the focus of this study.

3. Methods

A fresh ice block was suspended in a recirculating flume filled with room temperature (18–21°C) seawater (salinity $S \approx 32$ g kg^{-1}), such that it was unable to move, so the flow was equivalent to that observed in the iceberg's frame of reference (Figure 1). The experiments were conducted in a 300 × 500 cm tank, in which the flow speed could be continuously adjusted between 0 and 5 cm s^{-1}. The ice block had width 15 cm, length 10 cm, and immersed height 10 cm and was suspended in 20 cm of water. The ice was deaired and dyed so the spreading of meltwater could be observed. The ice block melted over an observation period of 15 min, and the SMR was calculated from the ice block mass difference scaled by its average surface area, as described in the supporting information. Note that this gives the total side and basal SMR, although basal melt makes a small contribution to the total mass loss (see supporting information).

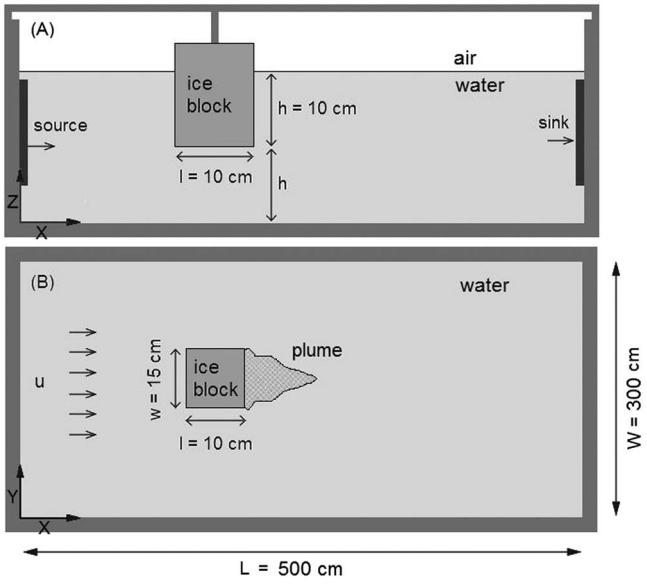

Figure 1. Schematic (not to scale) of the laboratory setup. (a) Side view of the ice block suspended in the working part of the flume. (b) Birdseye view of the ice block, with the surface expression of a downstream melt plume hatched.

In the absence of a background flow, melting occurs on all sides of the ice block, with the generation of rising meltwater plumes on each of the four vertical faces of the block. These melt plumes are also fed by buoyant basal melt and rapidly become turbulent for ice melting in room temperature water. They result in the surface pooling of meltwater, which spreads uniformly away from the ice block. By increasing the velocity of the flow past the ice block, we proceeded to test its influence on the melt plumes and SMR.

4. Results

We found that in general melt rate increases with flow speed, though nonlinearly. Qualitatively, we observed that melt plume behavior differs for low- and high-background flow speeds (Figure 2) and that this quantitatively impacts the dependence of SMR on flow speed (Figure 3). At low (<1.5 cm s^{-1}) flow speeds, the ice melted uniformly (Figure 2a), maintaining its rectangular profile save for a slight upward slope of the bottom face in the direction of the flow associated with vortex formation as water moved under the ice block. At these flow speeds, the meltwater rose uniformly in plumes around the ice block and spread in a surface layer. There was some sinking observed of filaments of ambient salt water

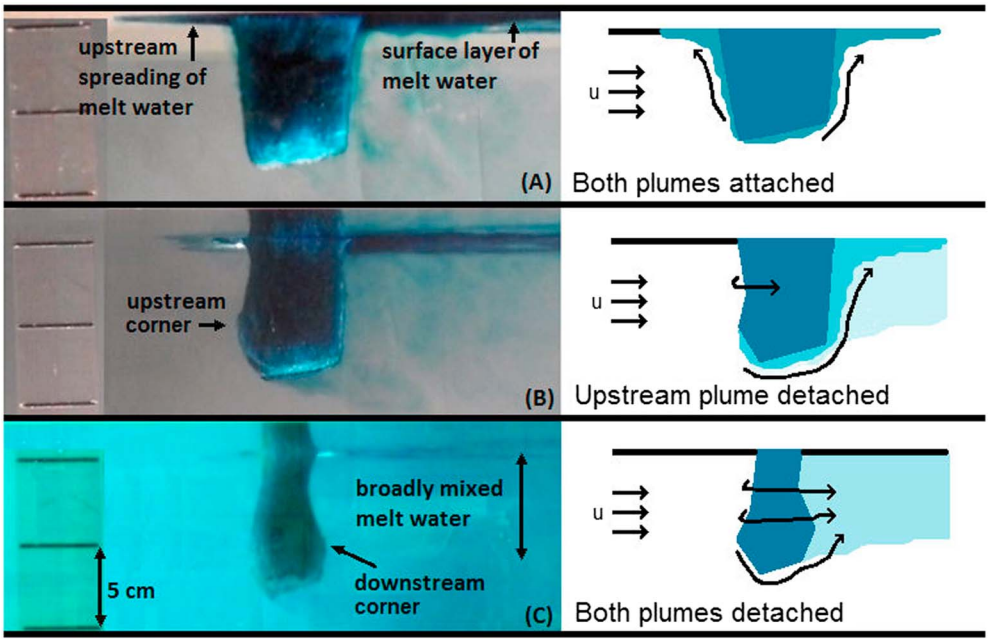

Figure 2. (left column) Side views of ice blocks after melting for 15 min in a homogeneous flow of (a) 0.5 cm s^{-1}, (b) 2 cm s^{-1}, and (c) 4.7 cm s^{-1}. Scale shown by ruler with 5 cm intervals. (right column) Schematic representations of left column.

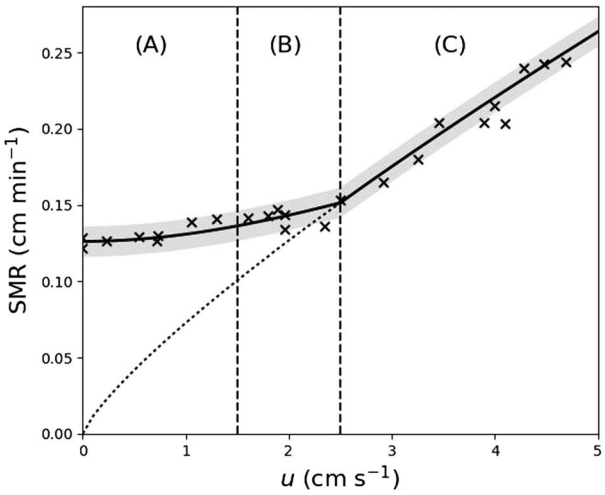

Figure 3. Dependence of SMR on flow speed, split into regions (a) both plumes attached, (b) upstream plume detached, downstream plume attached, and (c) both plumes detached. The parameterization proposed in equation (4) for an average ice temperature of −15°C is shown in black, and the shaded region depicts the experimental error (calculated from two standard deviations of three repeated experiments). The dashed extension of the detached regime curve is the standard parameterized value of $M_b = Ku^{0.8}(T_o - T_i)/L^{0.2}$ (where $K = 0.75$, $T_o = 20$°C, $T_i = -15$°C, and $L = 0.1$ m in the laboratory setting).

that had been more cooled conductively than freshened by the meltwater, but the majority of the motion was upward.

A qualitative change was observed in the profile of the ice block once the background flow speed exceeded 1.5 cm s^{-1}. A corner appeared on the upstream face of the ice block (Figure 2b), associated with the upstream melt plume being swept under and around the ice. The separation of the upstream plume meant that some of the meltwater no longer rose uniformly around the ice block to form a surface layer; rather, it began to mix with the ambient water and enter the water column also over the full draft of the ice block. When the background flow was increased to 2.5 cm s^{-1}, the downstream melt plume also fully separated from the ice block, and a second qualitative change was observed in the ice block profile. The upstream corner shifted lower on the ice block, and a downstream corner appeared, giving the melted ice block a pear-shaped appearance (Figure 2c). At flow speeds exceeding 2.5 cm s^{-1}, there was a high level of mixing between the melt and ambient water downstream of the ice block, as evidenced by the highly diluted dye downstream of the ice block, and no surface pooling of meltwater.

The change in melt plume behavior (from fully attached below 1.5 cm s^{-1} to fully detached above 2.5 cm s^{-1}) was associated with a distinct increase in the dependence of SMR on flow speed u (Figure 3). Physically, this results from the flow past the ice block influencing the ice block SMR in two ways. First, it modulates advective heat transport to the ice surface, resulting in the observed linear increase of SMR with u in each of the two melt plume regimes. Second, the background flow interacts with the melt plume as it rises, altering the angle the plume makes with the side of the ice block. If the plume is attached, the relatively cold water contained in the plume insulates the ice surface from the ambient water, so separating the plume from the ice enhances melting and causes the regime shift in Figure 3. We hypothesize that the regime transition (attached to detached plumes) occurs when the background flow speed u is of the same order of magnitude as the plume speed w. This is supported by the fact that the mean observed melt plume speed (calculated via feature-tracking) was 1.6 cm s^{-1}, with a two standard deviation range of $w \sim 1.2–2.2$ cm s^{-1}.

For tidewater glaciers it has been argued that increasing the strength (buoyancy flux) of the melt plume by supplying subglacial discharge enhances melting of the glacier face, as stronger (faster/wider) plumes entrain more warm ambient water and draw it toward the ice front [*Cenedese and Gatto*, 2016; *McConnochie and Kerr*, 2017]. However, in the case of icebergs it is possible to detach this melt plume entirely, allowing the ice to come directly in contact with the warm ambient waters, which are consistently renewed by the advecting background flow. So while those familiar with the tidewater glacier literature correctly associate stronger melt plumes with increased melting, an entirely absent melt plume results in even greater melting, provided the warm ambient water is continually renewed.

5. Parameterizing Side Melt

5.1. Model

Following our experimental findings, we update the iceberg side melt parameterization to be dependent on the melt plume behavior. In developing this parameterization, we assume that side melt dominates the

laboratory-measured SMR, as the aspect ratio of the ice blocks is such that the side area dominates (see supporting information). For the relative speed of the iceberg and the water less than the plume speed ($|u_o - u_i| < |w|$), when the melt plume is attached, the side melt rate is estimated using the melt parameterization due to forced convection, where the relevant speed, temperature, and length scale are the plume vertical speed $|w|$, the plume temperature T_p, and the iceberg draft D, respectively. For $|u_o - u_i| > |w|$, when the melt plume is detached, the side melt rate is instead estimated using the previous standard parameterization due to forced convection with ambient flow speed $|u_o - u_i|$ and ambient water temperature T_a past an iceberg of length L. We assume that the plume water is a mix of ambient water at $T = T_a$ and meltwater at $T = 0°C$, so $T_p = \alpha T_a$ with the fraction α of entrained water to meltwater proportional to the magnitude of the flow:

$$\alpha = \alpha_0 \sqrt{u^2 + w^2}. \tag{3}$$

With this model, the side melt rate M_s is

$$M_s = \begin{cases} \frac{K|w|^{0.8}(\alpha T_a - T_i)}{D^{0.2}} & |u_o - u_i| \le |w| \\ \frac{K|u_o - u_i|^{0.8}(T_a - T_i)}{L^{0.2}} & |u_o - u_i| > |w|, \end{cases} \tag{4}$$

where K is found to be approximately 0.58 for icebergs in the ocean, and 0.75 in the laboratory setting (see supporting information). With the laboratory-appropriate value of K, equation (4) gives the curve shown in Figure 3 for an average T_i of −15°C. Here α_0 is chosen to be $1/\sqrt{2}w$ to ensure continuity between the two regimes in the case $D = L$. This parameterization improves upon the previous standard parameterization of iceberg side melt (equation (2)) that does not account for the two dynamically different melt plume regimes, and unlike the three-equation parameterizations of melt (generally applied under ice shelves or along tidewater glacier faces) it considers the influence of a velocity that is normal to the plume direction, which is uniquely the case in iceberg side melt.

5.2. Application to Observations

We apply this updated parameterization of side melt to observations of 90 icebergs from Sermilik Fjord in southeastern Greenland, described in *Andres et al.* [2015] and *FitzMaurice et al.* [2016]. *FitzMaurice et al.* [2016] showed that these icebergs move predominantly with the vertical average of ocean currents over their draft. If currents are approximately uniform with depth, this means that the iceberg experiences very little relative velocity with the ocean and it will be in the attached plume regime at every depth. Alternatively, if there is a shear between the upper Polar Water and lower Atlantic Water layers in the fjord, the iceberg moves at the average of the layer speeds (weighted by how much of its draft is in each layer) and experiences a high relative velocity with the ocean, so it will be everywhere in the detached plume regime. These two scenarios (approximately barotropic and linear shear, respectively) are illustrated in Figure 4 and are representative of the majority of the relative velocity profiles felt by the icebergs in the observational record of *FitzMaurice et al.* [2016]. Thus, although the updated parameterization was developed for a homogeneous flow, we expect it to perform well in the real ocean as most icebergs fall into a single plume regime at every depth.

A further effect of vertical shear in the ambient current is that the parameterization will lead to an underestimate of SMR in regions where the relative speed transitions between the attached and detached regimes if an average ocean velocity is used (by the nonlinearity of equation (4)). We therefore proceed by applying the updated paramaterization to calculate the velocity and temperature-dependent SMR at every depth. We represent the thermal stratification of the fjord via an ocean temperature of 1°C above 180 m in the Polar Water layer, and 3°C below this depth in the Atlantic Water layer [*Straneo et al.*, 2011]. Note that the schematic representations of expected melt plume behavior (Figure 4) assume a weakly stratified ocean, or an iceberg entirely in the homogeneous top layer of the fjord. In the presence of a strong linear stratification the attached plume regime could lead to an intrusion at depth as opposed to a surface meltwater layer [*Huppert and Turner*, 1980].

When the melt plumes are detached, the updated parameterization is almost identical to the standard (equation (2)), with the only difference being the small term M_v. However, in the attached plume regime (which constitutes 40% of the icebergs in the observational record) the inclusion of the plume velocity in the side melt parameterization approximately doubles the mean side melt, from 0.06 m d^{-1} to 0.10 m d^{-1}, if the icebergs are assumed to have an aspect ratio equal to 1 and the ice temperature is the canonical value of $T_i = -4°C$ [*Bigg et al.*, 1997]. This parameterization is sensitive to the ice temperature, and if instead we assume

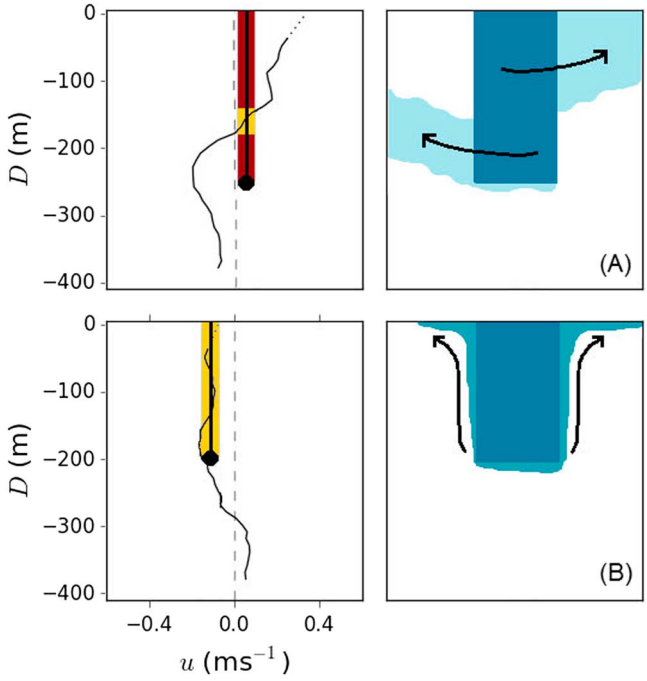

Figure 4. (left column) Sample profiles of along-fjord velocities felt by two icebergs in Sermilik Fjord, from *FitzMaurice et al.* [2016], in (a) a linearly sheared flow and (b) a barotropic flow. The solid vertical line indicates the iceberg draft and velocity, and the profile (thin black line) is the average ocean velocity during and leading up to the iceberg's observation, with the dashed extension of this profile illustrating the extrapolated velocity in the top 40 m of the water column. Depths at which the relative velocity of the ocean is sufficiently low that we would anticipate an attached plume are shaded in yellow, and depths where it is high enough for the melt plume to detach are shaded in red. We assume a plume speed of 0.05 m s^{-1} following the modeling of melting ice faces by *Sciascia et al.* [2013], which is consistent with the plume speed of 0.07 m s^{-1} observed next to a grounded iceberg by *Josberger and Neshyba* [1980]. (right column) Schematics of plume regimes for (Figure 4a) detached and (Figure 4b) attached plumes corresponding to linearly sheared flow and barotropic flows, respectively.

that $T_i = -15$°C as in *Lüthi and Funk* [2001], the mean side melt given by the updated (standard) parameterization for all icebergs increases to 0.40 m d^{-1} (0.34 m d^{-1}). Although when both regimes are considered the updated parameterization differs less from the standard parameterization than in the attached regime alone, this latter mean value from the updated parameterization agrees more closely with area-averaged SMRs estimated for icebergs in Sermilik Fjord by *Enderlin and Hamilton* [2014] of 0.39 m d^{-1}. Variations about the mean are caused by the proportion of each observed iceberg in either fjord layer being a function of the iceberg draft or observed icebergs being subject to different ocean velocity profiles. The side SMR suggested by this parameterization at $T_i = -15$°C results in 146 m of side melt per year, consistent with iceberg tracking studies around Greenland [*Sutherland et al.*, 2014] that indicate icebergs ranging in horizontal size 100 to >500 m survive for at least 80 days in Sermilik Fjord.

6. Discussion

We began by noting the importance of understanding how icebergs melt in different ocean conditions and where this meltwater goes in the water column for predictions of future ocean circulation and biological productivity. A further consideration relates to the observed increase in Antarctic sea ice extent over the last few decades [*Hobbs et al.*, 2016], despite rising temperatures around Antarctica. One hypothesized that mechanism contributing to this trend is an increased discharge of freshwater into the Southern Ocean from ice sheet and iceberg melt [*Bintanja et al.*, 2013; *Merino et al.*, 2016; *Stern et al.*, 2016], which can promote sea ice growth, assuming meltwater is deposited in a fresh surface layer and suppresses the upwelling of heat. If iceberg meltwater were instead to enter the water column below the surface, the mixing with warmer water at depth could act to suppress sea ice growth. It is thus of interest to determine whether icebergs generally fall into a regime where their meltwater is channeled directly to the surface via attached side melt plumes, or if meltwater mixes over a broader layer in detached melt plumes. Figure 4 shows that some realistic icebergs are likely in the detached plume regime, implying that their meltwater mixes in the downstream water column over the iceberg draft, while others likely distribute their meltwater in a more undiluted surface layer (or in an intermediate intrusion layer in the case of a strongly stratified ocean) due to having side-attached melt plumes. This motivates the direct observation of iceberg melt plumes to determine their behavior in the real ocean.

In the laboratory, it was found that at flow speeds less than $\sim 0.4|w|$, meltwater may spread at the surface upstream of the ice block as well as downstream (Figure 2a). This agrees with satellite observations of enhanced chlorophyll concentrations (associated with upwelling of nutrient-rich water in melt plumes) around giant icebergs in the Southern Ocean. *Duprat et al.* [2016] observed high chlorophyll concentrations

upstream and downstream of large tabular icebergs; an initially counterintuitive result if one believes meltwater is carried downstream with the flow and there is relatively little vertical shear in the flow. Our results suggest that in low-relative velocities (when the iceberg moves predominantly with the ocean currents) it may indeed be possible for meltwater to spread against the background flow due to the buoyancy-driven gravity current generated by surface pooling of meltwater.

While our study has highlighted the importance of the flow past an iceberg on the iceberg side melt due to the ability of the background flow to interact with icebergs' melt plumes, further work remains. It is anticipated that the aspect ratio of icebergs might influence the strength of side melt plumes if these are fed by basal melt. Consequently, Greenlandic and Antarctic icebergs, which typically have very different aspect ratios, may fall into different melt regimes when subject to the same relative ocean velocity. Furthermore, in this study we have only considered relative velocities and background temperature and salinity profiles that are uniform with depth. How a sheared flow interacts with melt plumes to affect the side melting of icebergs will be the focus of a future contribution. The behavior of melt plumes in a stratified shear flow is also a topic of interest if we are to fully understand the iceberg side melt in a stratified ocean.

7. Conclusions

Novel laboratory experiments suggested that for an ice block melting in an nonstratified homogeneous flow, melt plumes are side attached when the plume velocity is larger than the relative velocity of the flow past the iceberg and are detached when the relative velocity becomes larger than the plume velocity. The existence of these different regimes results in a nonlinear dependence of the iceberg melt rate on relative velocity. A further important effect of relative velocity on an ice block's melting is where the meltwater is distributed. At speeds low enough that the melt plumes are attached to the ice, the meltwater spreads in an almost undiluted surface layer. At speeds high enough that the melt plumes are detached, the meltwater is diluted downstream of the ice block and distributed over the ice block draft.

We hypothesize that the transition between attached and detached plume regimes occurs when the magnitude of the relative velocity is of the same order as the melt plume vertical velocity. With this assumption, our updated plume-dependent melt rate parameterization may be scaled up and applied to observed icebergs. For a record of 90 icebergs with concurrent ocean velocity data in Sermilik Fjord, southeastern Greenland, the application of this updated parameterization doubles the mean side melt in the attached plume regime, improving agreement with local observations of iceberg melt rates. It is further shown that icebergs may exist in both the attached and detached plume regimes, which may influence whether their meltwater is distributed at the surface or mixed at depth. This motivates further observation of iceberg melt plumes in the ocean to determine their behavior in flows that may be complicated by the presence of shear and background stratification.

Acknowledgments
We acknowledge M. Andres for collection of the observational record of icebergs from Sermilik Fjord (data and code available at heatandice.whoi.edu). The authors thank A. Jensen for his invaluable technical expertise in constructing the experimental apparatus and for his able assistance in the laboratory. A.F. was supported by NA14OAR4320106 from the National Oceanic and Atmospheric Administration, U.S. Department of Commerce. The statements, findings, conclusions, and recommendations are those of the authors and do not necessarily reflect the views of the National Oceanic and Atmospheric Administration, or the U.S. Department of Commerce. C.C. was supported by NSF OCE-1434041 and OCE-1658079, and F.S. was supported by NSF PLR-1332911 and OCE-1434041. We thank two anonymous reviewers who provided constructive feedback.

References

Andres, M., A. Silvano, F. Straneo, and D. R. Watts (2015), Icebergs and sea ice detected with inverted echo sounders, *J. Atmos. Oceanic Technol.*, *32*(5), 1042–1057.

Bamber, J. L., and W. P. Aspinall (2013), An expert judgement assessment of future sea level rise from the ice sheets, *Nat. Clim. Change*, *3*(4), 424–427.

Bigg, G. R., M. R. Wadley, D. P. Stevens, and J. A. Johnson (1997), Modelling the dynamics and thermodynamics of icebergs, *Cold Reg. Sci. Technol.*, *26*(2), 113–135.

Bintanja, R., G. J. Van Oldenborgh, S. S. Drijfhout, B. Wouters, and C. A. Katsman (2013), Important role for ocean warming and increased ice-shelf melt in Antarctic sea-ice expansion, *Nat. Geosci.*, *6*(5), 376–379.

Böning, C. W., E. Behrens, A. Biastoch, K. Getzlaff, and J. L. Bamber (2016), Emerging impact of Greenland meltwater on deepwater formation in the North Atlantic Ocean, *Nat. Geosci.*, *9*, 523–527.

Budd, W., T. Jacka, and V. Morgan (1980), Antarctic iceberg melt rates derived from size distributions and movement rates, *Ann. Glaciol.*, *1*, 103–112.

Cenedese, C., and V. M. Gatto (2016), Impact of a localized source of subglacial discharge on the heat flux and submarine melting of a tidewater glacier: A laboratory study, *J. Phys. Oceanogr.*, *46*(10), 3155–3163.

Duprat, L. P. A. M., G. R. Bigg, and D. J. Wilton (2016), Enhanced Southern Ocean marine productivity due to fertilization by giant icebergs, *Nat. Geosci.*, *9*, 219–221.

El-Tahan, M., S. Venkatesh, and H. El-Tahan (1987), Validation and quantitative assessment of the deterioration mechanisms of Arctic icebergs, *J. Offshore Mech. Arct. Eng.*, *109*(1), 102–108.

Enderlin, E. M., and G. S. Hamilton (2014), Estimates of iceberg submarine melting from high-resolution digital elevation models: Application to Sermilik Fjord, East Greenland, *J. Glaciol.*, *60*(224), 1111–1116.

Enderlin, E. M., G. S. Hamilton, F. Straneo, and D. A. Sutherland (2016), Iceberg meltwater fluxes dominate the freshwater budget in Greenland's iceberg-congested glacial fjords, *Geophys. Res. Lett.*, *43*, 11,287–11,294, doi:10.1002/2016GL070718.

FitzMaurice, A., F. Straneo, C. Cenedese, and M. Andres (2016), Effect of a sheared flow on iceberg motion and melting, *Geophys. Res. Lett.*, *43*, 12,520–12,527, doi:10.1002/2016GL071602.
Gade, H. G. (1993), When ice melts in sea water: A review, *Atmos. Ocean*, *31*(1), 139–165.
Gladstone, R. M., G. R. Bigg, and K. W. Nicholls (2001), Iceberg trajectory modeling and meltwater injection in the Southern Ocean, *J. Geophys. Res.*, *106*(C9), 19,903–19,915.
Helly, J., R. Kaufmann, G. Stephenson, and M. Vernet (2010), Cooling, dilution and mixing of ocean water by free-drifting icebergs in the Weddell Sea, *Deep Sea Res., Part II*, *58*(11–12), 1346–1363.
Hobbs, W. R., R. Massom, S. Stammerjohn, P. Reid, G. Williams, and W. Meier (2016), A review of recent changes in Southern Ocean sea ice, their drivers and forcings, *Global Planet. Change*, *143*, 228–250.
Hobson, B. W., A. D. Sherman, and P. R. McGill (2011), Imaging and sampling beneath free-drifting icebergs with a remotely operated vehicle, *Deep Sea Res., Part II*, *58*(11), 1311–1317.
Holland, D., and A. Jenkins (1999), Modeling thermodynamic ice-ocean interactions at the base of an ice shelf, *J. Phys. Oceanogr.*, *29*(8), 1787–1800.
Huppert, H. E., and J. S. Turner (1980), Ice blocks melting into a salinity gradient, *J. Fluid Mech.*, *100*(2), 367–384.
Josberger, E., and S. Neshyba (1980), Iceberg melt-driven convection inferred from field measurements of temperature, *Ann. Glaciol.*, *1*, 113–117.
Kubat, I., M. Sayed, S. Savage, T. Carrieres, and G. Crocker (2007), An operational iceberg deterioration model, paper presented at 17th International Offshore and Polar Engineering Conference, pp. 652–657, Lisbon, Portugal, 1–6 July.
Lüthi, M. P., and M. Funk (2001), Modelling heat flow in a cold, high-altitude glacier: Interpretation of measurements from Colle Gnifetti, Swiss Alps, *J. Glaciol.*, *47*(157), 314–324.
Martin, T., and A. Adcroft (2010), Parameterizing the fresh-water flux from land ice to ocean with interactive icebergs in a coupled climate model, *Ocean Modell.*, *34*(3–4), 111–124.
McConnochie, C. D., and R. C. Kerr (2016), The turbulent wall plume from a vertically distributed source of buoyancy, *J. Fluid Mech.*, *787*, 237–253.
McConnochie, C. D., and R. C. Kerr (2017), Enhanced ablation of a vertical ice wall due to an external freshwater plume, *J. Fluid Mech.*, *810*, 429–447.
Merino, N., J. Le Sommer, G. Durand, N. C. Jourdain, G. Madec, P. Mathiot, and J. Tournadre (2016), Antarctic icebergs melt over the Southern Ocean: Climatology and impact on sea ice, *Ocean Modell.*, *104*, 99–110.
Neshyba, S., and E. G. Josberger (1980), On the estimation of Antarctic iceberg melt rate, *J. Phys. Oceanogr.*, *10*(10), 1681–1685.
Rignot, E., I. Velicogna, M. R. Van den Broeke, A. Monaghan, and J. T. M. Lenaerts (2011), Acceleration of the contribution of the Greenland and Antarctic ice sheets to sea level rise, *Geophys. Res. Lett.*, *38*, L05503, doi:10.1029/2011GL046583.
Russell-Head, D. (1980), The melting of free-drifting icebergs, *Ann. Glaciol.*, *1*, 119–122.
Savage, S. B. (2001), Aspects of iceberg deterioration and drift, *Geomorphol. Fluid Mech.*, *582*, 279–318.
Sciascia, R., F. Straneo, C. Cenedese, and P. Heimbach (2013), Seasonal variability of submarine melt rate and circulation in an East Greenland fjord, *J. Geophys. Res. Oceans*, *118*, 2492–2506, doi:10.1002/jgrc.20142.
Sgubin, G., D. Swingedouw, S. Drijfhout, Y. Mary, and A. Bennabi (2017), Abrupt cooling over the North Atlantic in modern climate models, *Nat. Commun.*, *8*, 14375, doi:10.1038/ncomms14375.
Smith, K. L., B. H. Robison, J. J. Helly, R. S. Kaufmann, H. A. Ruhl, T. J. Shaw, B. S. Twining, and M. Vernet (2007), Free-drifting icebergs: Hot spots of chemical and biological enrichment in the Weddell Sea, *Science*, *317*(5837), 478–482.
Stephenson, G. R., J. Sprintall, S. T. Gille, M. Vernet, J. J. Helly, and R. S. Kaufmann (2015), Subsurface melting of a free-floating Antarctic iceberg, *Deep Sea Res., Part II*, *58*(11), 1336–1345.
Stern, A. A., A. Adcroft, and O. Sergienko (2016), The effects of Antarctic iceberg calving-size distribution in a global climate model, *J. Geophys. Res. Oceans*, *121*, 5773–5788, doi:10.1002/2016JC011835.
Straneo, F., R. G. Curry, D. A. Sutherland, G. S. Hamilton, C. Cenedese, K. Våge, and L. A. Stearns (2011), Impact of fjord dynamics and glacial runoff on the circulation near Helheim Glacier, *Nat. Geosci.*, *4*(5), 322–327.
Sutherland, D. A., G. Roth, G. S. Hamilton, S. Mernild, L. A. Stearns, and F. Straneo (2014), Quantifying flow regimes in a Greenland glacial fjord using iceberg drifters, *Geophys. Res. Lett.*, *41*, 8411–8420, doi:10.1002/2014GL062256.
Weeks, W. F., and W. J. Campbell (1973), Icebergs as a fresh-water source: An appraisal, *J. Glaciol.*, *12*(65), 207–233.
Yankovsky, A., and I. Yashayaev (2014), Surface buoyant plumes from melting icebergs in the Labrador Sea, *Deep Sea Res., Part I*, *91*, 1–9.